

$W + 3$ jet production at the LHC as a signal or background

Kirill Melnikov

*Department of Physics and Astronomy,
Johns Hopkins University, Baltimore, MD, USA*

Giulia Zanderighi

*Rudolf Peierls Centre for Theoretical Physics,
1 Keble Road, University of Oxford, UK*

We discuss the production of W bosons in association with three jets at the LHC. We investigate how next-to-leading order QCD corrections modify basic kinematic distributions of jets and leptons. We also address the magnitude of NLO QCD effects in $W + 3$ jet observables, relevant for SUSY searches at the LHC.

I. INTRODUCTION

A good understanding of complicated multi-particle processes is important for the LHC physics. To achieve this goal it is useful to have next-to-leading order (NLO) QCD predictions for such processes (see e.g. Ref. [1]). In the past, *three* final state particles was the highest multiplicity for which NLO QCD computations were feasible, but this changed this year when four groups [2, 3, 4, 5, 6, 7, 8] reported first results on NLO QCD corrections to processes with *four* particles in the final state. To arrive at these results a variety of methods including highly-refined Passarino-Veltman reduction algorithm [9, 10], Ossola-Pittau-Papadopoulos (OPP) method [11, 12] and unitarity techniques [13, 14, 15, 16, 17, 18] were used. Successful completion of these computations and a large number of one-loop amplitudes with six and more external particles computed recently [19, 20, 21, 22, 23, 24, 25], provides a proof of principle that reliable description of many $2 \rightarrow 4$ processes is now within reach.

A major reason for extending leading order results to next-to-leading order is a significant reduction of the unphysical dependence on factorization and renormalization scales in NLO QCD cross sections and distributions. Such reduction is very important, especially for high multiplicity processes, where the unphysical dependence on scales can be significant. Indeed, for such processes, the scale dependence is amplified by the high power of the strong coupling constant. For a cross-section involving n jets $\sigma_n \sim \alpha_s^n(\mu)$, so that small changes in the renormalization scale μ lead to large changes in the corresponding cross sections

$$\mu \frac{\partial \sigma_n}{\partial \mu} \sim -2n\beta_0 \alpha_s \sigma_n, \quad \beta_0 = (11N_c - 2n_f)/(12\pi). \quad (1)$$

There are many cases where NLO computations reduce

the dependence of cross sections on unphysical scales to 10 – 20% which, given typical cross section uncertainties at leading order (LO) of about 50%, is a great success. However, even if such scale-independence is observed for the total-cross section, it is not always possible to claim that a particular process is described reliably, for the purpose of LHC phenomenology. The reason is the dual role that many complicated processes at the LHC will play. Indeed, depending on the cuts on the final states, processes that involve e.g. top quarks and/or electroweak gauge bosons and QCD jets are treated as either primary signals or unwanted backgrounds and very different cuts are applied to final states in the two cases. We will refer generically to these cuts as “signal” or “background” cuts, respectively ¹ These cuts force final state particles to live in different regions of phase-space, so that *a priori* it is not possible to relate QCD corrections to the same process subject to either “signal” or “background” cuts.

A candidate procedure for dealing with LHC processes which have this dual role is as follows. One starts the study of these processes by applying signal cuts and using the resultant data set to refine the theoretical tools, e.g. Monte Carlo event generators. Once a good understanding of a given process is achieved with signal cuts, one uses the refined tools to extrapolate to a different kinematic situation, specified by the background cuts. Unfortunately, the reliability of this extrapolation is not assured. The purpose of applying the background cuts

¹ Since we are mainly concerned with the process $W + 3$ jets, we call “signal cuts” the ones where this process is considered a signal, and “background cuts” the ones for which this process is an unwanted background to some other New Physics signal. We caution the reader that these terms are often used in the literature in exactly the opposite way.

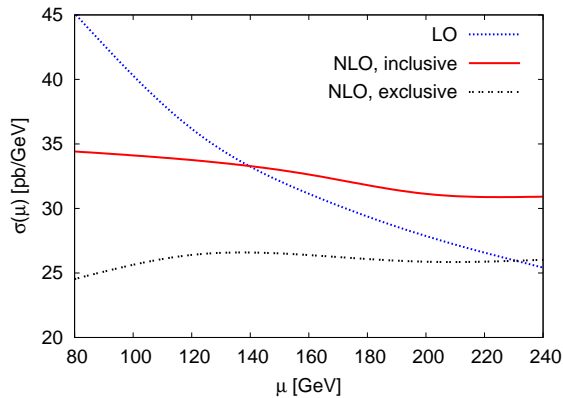


FIG. 1: The dependence of the $W^+ + 3$ jet inclusive production cross section at the LHC on the factorization and renormalization scale μ . All cuts and parameters are described in the text. The leading color adjustment procedure is applied.

is to suppress, as far as possible, the very kinematic configurations that are allowed by signal cuts. Therefore, such an extrapolation can only work if the influence of kinematics on QCD radiative effects is correctly captured by the available tools. Since only relatively simple theoretical tools, such as leading order parton integrators or parton showers, are currently available for complicated final states, the modeling of the radiative effects is only approximate. On the other hand, if a NLO QCD computation is available, such an extrapolation can be done with a smaller ambiguity since all the relevant scales are generated dynamically in NLO computations, largely independent of the choices made initially. For cases with complicated kinematics, this is clearly indispensable.

In this paper we discuss and illustrate this issue, taking the production of W bosons in association with three jets at the LHC as an example. For definiteness, we choose to consider proton-proton collisions at $\sqrt{s} = 10$ TeV [26]. However, we do not aim to describe $W + 3$ jet production at the LHC in all possible detail, since knowledge of the exact experimental setup would be required. Instead, we look for and try to understand differences between NLO and LO QCD results for basic observables, for the case of signal cuts. We point out that it is not always clear which leading order predictions should be used in those comparisons since different choices of renormalization and factorization scales affect the leading order predictions strongly. We therefore compare our results to a variety of leading order predictions including most advanced ones, where matrix element computations are matched to parton showers.

We note that NLO QCD corrections to $W+3$ jet production at the LHC have been studied in great detail recently in Ref. [6], mostly for signal cuts. We have checked a number of results for W^\pm production cross-sections at the LHC, reported in that reference, and found agreement within a few percent in all cases con-

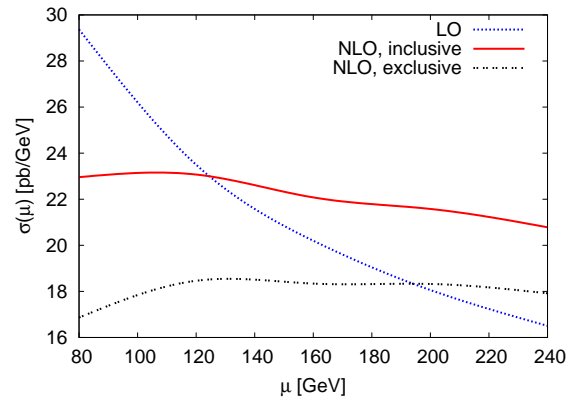


FIG. 2: The dependence of the $W^- + 3$ jet inclusive production cross section at the LHC on the factorization and renormalization scale μ . All cuts and parameters are described in the text. The leading color adjustment procedure is applied.

sidered. These small differences are compatible with the fact that our calculation employs the leading color approximation with color adjustment procedure, explained in detail in Ref. [5], whereas computation in Ref. [6] accounts for complete color dependence.

We also discuss QCD corrections to *background cuts*, studied by the ATLAS [27, 28, 29] and CMS collaborations [30, 31] for SUSY searches at the LHC. Such analyses often assume that Standard Model backgrounds can be measured in SUSY-free regions to fix normalizations and then employ LO computations to extrapolate to kinematic regions where supersymmetric signal is expected. Hence, an implicit assumption in those analyses is that LO distributions have correct shapes and that higher-order QCD effects provide a kinematic-independent renormalization. We are now in position to check these assumptions with the explicit NLO QCD computation of $W + 3$ jet process for typical ATLAS and CMS cuts.

The remainder of the paper is organized as follows. In Section II, we discuss $W + 3$ jet production for signal cuts at the LHC. In Section III we study $W + 3$ jet production as a background to SUSY searches for two typical sets of cuts close to those suggested by the ATLAS and CMS collaborations. In Section IV we present our conclusions.

II. STUDY OF $W + 3$ JET PROCESS

In this Section, we discuss NLO QCD effects in $W + 3$ jet production for a set of cuts, designed to study the W production in association with jets. We follow Ref. [5] closely and perform calculations in the leading color approximation. The calculation relies heavily on the framework provided by MCFM [32] and uses one-loop amplitudes computed in [22]. We employ the Catani-Seymour dipole subtraction [33] to compute real emission correc-

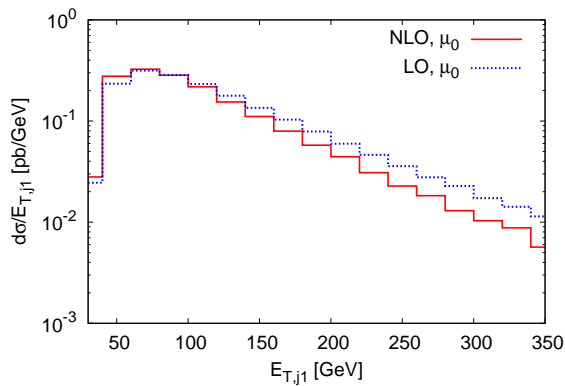


FIG. 3: The transverse momentum distribution of the leading jet for $W^+ + 3$ jet inclusive production cross section at the LHC. All cuts and parameters are described in the text. The leading color adjustment procedure is applied.

tion; details of our implementation are given in [4]. We use the leading color adjustment procedure described in that paper to correct for deficiencies of the leading color approximation, to the extent possible. We note that production cross-sections for W^+ and W^- at the LHC are not the same; we have chosen to discuss the case of W^+ production almost everywhere in this paper. We do, however, show results for the $W^- + 3$ jet production cross-section at the LHC in dependence of factorization and renormalization scales.

We begin by summarizing all the relevant cuts and input parameters that are employed in the computation. We take the LHC center-of-mass energy to be 10 TeV. We require that the transverse momentum and pseudorapidity of the three jets satisfy $p_{T,j} > 30$ GeV and $|\eta_j| < 3$. We consider the leptonic decay of the W to electron (or muon) and employ the following restrictions on lepton transverse momentum, missing transverse energy, lepton rapidity and W-boson transverse mass, $p_{T,e} > 20$ GeV, $\cancel{E}_T > 15$ GeV, $|\eta_e| < 2.4$, $M_T^W > 30$ GeV. We do not apply an isolation cut on the leptons. To define jets, we use the SIScone jet-algorithm [34] with $R = \sqrt{\Delta\eta^2 + \Delta\phi^2} = 0.5$ and merging parameter $f = 0.5$.

We consider the production of *on-shell* W^+ bosons, that decay into a pair of massless leptons. Finite width effects are about 1%; they tend to decrease the cross section. The CKM matrix is set equal to the identity matrix; this *reduces* the $W + 3$ jet production cross section at the LHC by less than 1%. All quarks, with the exception of the top quark, are considered massless. The top quark is considered infinitely heavy and its contribution is neglected. The mass of the W boson is taken to be $m_W = 80.419$ GeV; its couplings to fermions are obtained from $\alpha_{\text{QED}}(m_Z) = 1/128.802$ and $\sin^2 \theta_W = 0.230$. We use CTEQ6L parton distribution functions for leading order and CTEQ6M for next-to-leading order computations [35, 36]. Note that we do not include the factor

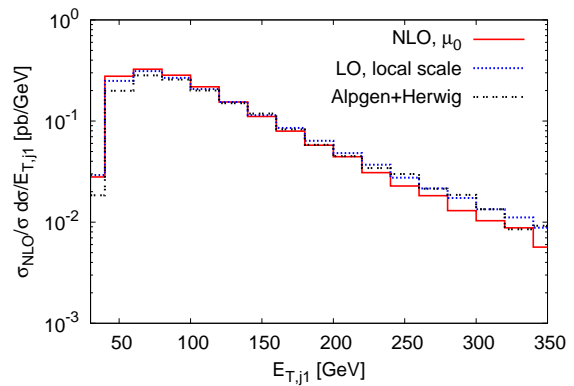


FIG. 4: The transverse momentum distribution of the leading jet for $W^+ + 3$ jet inclusive production cross section at the LHC. All cuts and parameters are described in the text. The leading color adjustment procedure is applied. All LO distributions are rescaled by constant factor, to ensure that the LO and NLO normalizations coincide.

$\text{Br}(W \rightarrow l\nu_l)$ in the results for cross-sections quoted below.

We first discuss results for total cross sections. We set renormalization and factorization scales μ to $\mu = [80, 120, 160, 200, 240]$ GeV and calculate the cross-sections with the cuts defined at the beginning of this Section. The result of the calculation is illustrated in Fig.1. For full-color leading order cross section we find

$$\sigma_{W^{++}\geq 3j}^{\text{LO,FC}} = 35(10) \text{ pb}, \quad (2)$$

where the ± 10 pb uncertainty from scale variation is shown in brackets. Calculating the same cross-section in the leading color approximation, we find the leading color adjustment parameter

$$\mathcal{R} = \sigma_{W^{++}\geq 3j}^{\text{LO,FC}} / \sigma_{W^{++}\geq 3j}^{\text{LO,LC}} = 0.940(5), \quad (3)$$

where the uncertainty indicates changes in this ratio that we observe when we change factorization/renormalization scales chosen in leading order computations or cuts on the final state particles. We also find that the \mathcal{R} ratio for the W^- production is the same as for the W^+ . Since \mathcal{R} does not depend in any significant way on the details of the process, applied cuts and chosen scales, we use the central value for \mathcal{R} given in Eq.(3) in what follows.

At NLO we obtain the *adjusted leading-color* inclusive cross-section, $\sigma_{W^{++}\geq 3j}^{\text{NLO,aLC}}(\text{incl}) = \mathcal{R} \cdot \sigma_{W^{++}\geq 3j}^{\text{NLO,LC}}(\text{incl})$,

$$\sigma_{W^{++}\geq 3j}^{\text{NLO,aLC}}(\text{incl}) = 32.4(1.5) \text{ pb}. \quad (4)$$

This result implies (see Fig.1) that for our choice of cuts and input parameters, NLO QCD corrections to the inclusive cross-section are very moderate for $\mu \sim 140 - 160$ GeV. We also observe a remarkable reduction

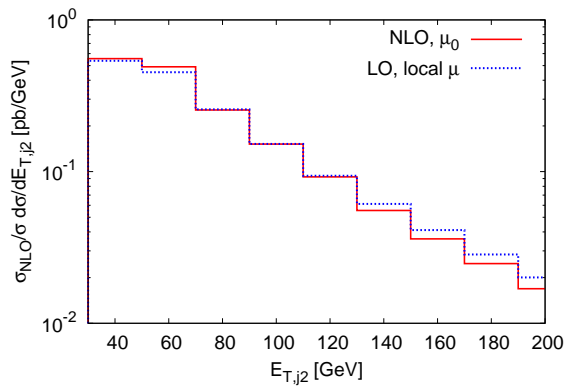


FIG. 5: The transverse momentum distribution of the second hardest jet in $W^+ + 3$ jet production at the LHC. All cuts and parameters are described in the text. The leading color adjustment procedure is applied. The LO distribution is rescaled by constant factor, to ensure that the LO and NLO normalizations coincide.

in scale dependence from more than $\pm 30\%$ at leading order to only $\pm 5\%$ at NLO. While corrections to the *exclusive cross-section* are larger for similar values of μ , the scale independence of the exclusive NLO cross-section is similar to the inclusive one. In Fig.2 the cross-section for $W^- + 3$ jet production is shown in dependence on the factorization and renormalization scales. The cross section is smaller in this case, while the stabilization of scale dependence that occurs at next-to-leading order is very similar for W^- and W^+ production cross-sections.

Given that NLO QCD corrections to the total cross sections are small, it is tempting to surmise that the corrections to kinematic distributions should also be insignificant. As we will now show, the actual situation is more complex. We consider kinematic distributions for the inclusive $W^+ + 3$ jet production. We choose to show the NLO distributions for the *dynamical* scale $\mu_0 = \sqrt{p_{T,W}^2 + m_W^2}$, where $p_{T,W}$ is the transverse momentum of the W boson as done e.g. in [37]. We note that for such a scale the LO cross-section is $\sigma_{W^+ + \geq 3j}^{\text{LO}} = 37.6$ pb and the adjusted leading color NLO cross-section is $\sigma_{W^+ + \geq 3j}^{\text{NLO,aLC}} = 34.2$ pb, consistent with Eq. (4) within the indicated uncertainties. The radiative corrections to $W + 3$ jet production cross-section at scale μ_0 are therefore small, about -10% . For the following discussion, scale choices in NLO computations are not very important since, as it turns out, *shapes* of NLO distributions are fairly insensitive to them.

We begin by studying the transverse momentum distribution of the leading jet. In Fig. 3 we compare NLO and LO predictions for scale μ_0 . We find that the NLO QCD corrections change the shape of this distribution – the leading order distribution underestimates the NLO result at small values of the transverse energy by about 30 percent and systematically exceeds the NLO result for

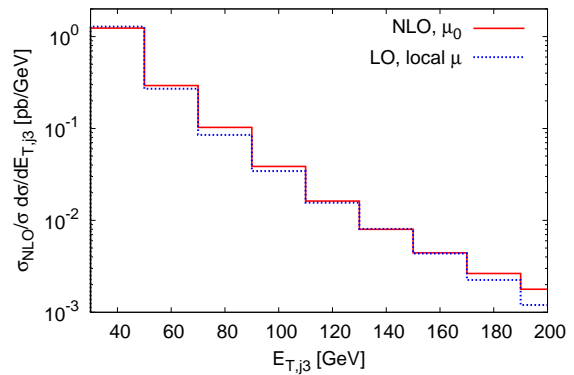


FIG. 6: The transverse momentum distribution of the third hardest jet in $W^+ + 3$ jet production at the LHC. All cuts and parameters are described in the text. The leading color adjustment procedure is applied. The LO distribution is rescaled by constant factor, to ensure that the LO and NLO normalizations coincide.

higher values of the transverse energy. A similar feature is observed in other distributions related to jet transverse momenta if the NLO result is compared to LO predictions with the scale μ_0 .

The origin of these shape changes was recently discussed in Ref. [38] using soft-collinear effective theory and in Refs. [5, 7] in connection with NLO QCD computations for $W + 3$ jets production at the Tevatron and the LHC. Here, we recapitulate the explanation of the inadequacy of the scale μ_0 given in Ref. [5]. This inadequacy is related to two facts: a) in the region where the jets have large transverse momentum, the W -boson transverse momentum spectrum is softer than that of the jets; b) the probability of parton branching is determined by the relative transverse momentum of the two daughter partons produced in that branching; such transverse momentum should be the appropriate scale for the strong coupling constant. When these two facts are combined, one is led to the conclusion that in the kinematic region where the jets have large transverse momenta, the use of $\alpha_s(\mu_0)$ in LO computations overestimates the cross section. At next-to-leading order, the appropriate scale for the strong coupling constant $\mu \sim p_{T,j} \gg \mu_0$ is generated dynamically and the cross section in that region becomes smaller.

Is it possible to account for the shape modifications by more sophisticated LO computations? The affirmative answer to this question was given in Refs. [7, 38], where particular choices of scales set by e.g. the hadronic invariant mass or total transverse energy in an event, were advocated. It should be emphasized, however, that the idea to employ scales of the strong coupling that are determined from local kinematics on an event-by-event basis is not new since it is central to both parton showers and advanced leading order computations that employ matrix elements and parton shower matching [39].

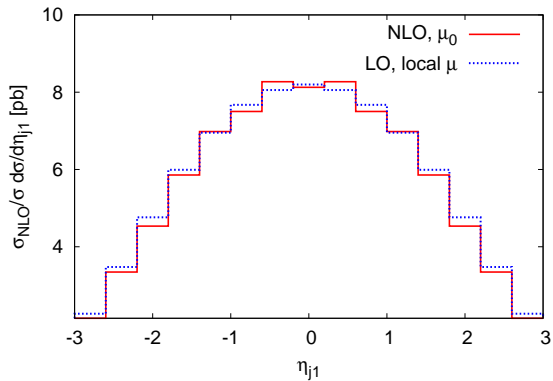


FIG. 7: The rapidity distribution of the leading jet for $W^+ + 3$ jet inclusive production cross section at the LHC. All cuts and parameters are described in the text. The leading color adjustment procedure is applied. The LO distribution is rescaled by constant factor, to ensure that the LO and NLO normalizations coincide.

Since such “local” scales capture the kinematics of complicated events correctly, it is conceivable that they produce shapes that are close to exact NLO results. We show the comparison of the NLO prediction with two leading order results in Fig. 4.

One LO distribution is obtained by following the MLM procedure whose application to $W + 3$ jet production is described in Ref. [37]. The MLM procedure and its close relative the CKKW algorithm [39] are the most advanced techniques available currently for leading order predictions, so it is interesting to see how it compares with NLO computations. We use Alpgen [40] to generate unweighted events that are matched to the Herwig [41] parton shower. We produce hard events with up to five QCD partons in the final state with Alpgen, using a transverse momentum cut of $p_{tj,\min} = 20$ (25) GeV and a separation parameter $d_{rj} = 0.35$ (0.45) [40]. To shower the hard events with Herwig we used $R_{\text{clus}} = d_{rj}$ and $E_{t,\text{clus}} = p_{tj,\min}$ as matching parameters for the MLM prescription [40]. We find that results are fairly independent of the cuts used in the generation of the hard events and that samples with five hard partons contribute little. This indicates that hard samples with yet higher multiplicity can be safely neglected.

The other LO prediction shown in Fig. 4 is our implementation of the local scales in the strong coupling constant; it is close in spirit to the re-weighting part of the CKKW procedure [39]. To this end, for a given LO partonic event that passes jet cuts, we cluster partons according to the measure given by k_{\perp} -jet algorithm². A

² We note that the jet cuts can be defined with any jet algorithm; the k_{\perp} -algorithm is only used to reconstruct the event branching history.

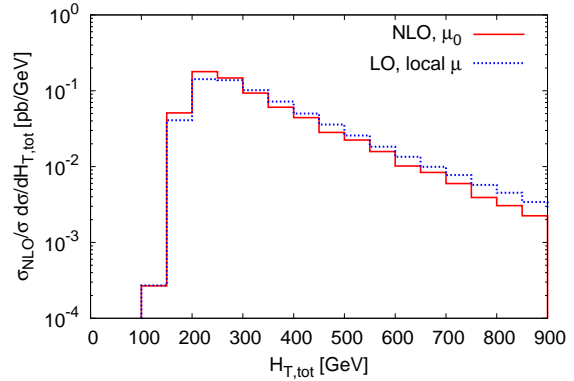


FIG. 8: The total transverse energy distribution for $W^+ + 3$ jet inclusive production cross section at the LHC. All cuts and parameters are described in the text. The leading color adjustment procedure is applied. The LO distribution is rescaled by constant factor, to ensure that the LO and NLO normalizations coincide.

repeated clustering gives us a “branching history” that can be associated with the event; at each branching the scale of the strong coupling constant is chosen as the relative momentum of two daughters in the branching. We will refer to scales of the strong coupling constant chosen by this algorithm as “local” scales. Note that this procedure is strictly a simple way to set scales of the strong coupling constant to reasonable values in $W + 5$ parton leading order matrix elements. In doing so, we do not try to combine matrix elements of different multiplicities nor do we attempt to shower leading order partonic configuration. Differences between distributions produced with Alpgen and with the local scale procedure give an idea of the importance of the parton shower and Sudakov re-weighting.

We point out that such modifications of leading order computations may lead to large changes in the cross-sections. For example, Alpgen cross-section is ~ 22 pb and the local scale cross-section is ~ 47 pb, to be compared with ~ 33 pb NLO cross-section. However, the normalization of cross-sections is a hard problem where next-to-leading computations or direct normalization to data are the only known solutions. To separate issues of normalization from the shape, we normalize all leading order results in Fig. 4 to the NLO cross-section. We observe that both the Alpgen+Herwig distribution and the local scale distribution describe the NLO result fairly well. Also, the proximity between the shapes of the two leading order results tells us that parton shower does relatively little to alter the shape of the distribution.

We find that these observations are generic: leading order computations obtained with either Alpgen+Herwig or local scales are similar and they work reasonably well in reproducing shapes of NLO distributions. We believe this is important conclusion, especially in the case of Alpgen+Herwig since those programs are used by experi-

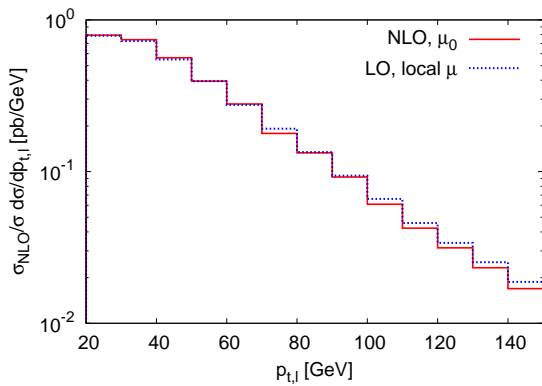


FIG. 9: The transverse momentum distribution of the charged lepton for $W^+ + 3$ jet inclusive production cross section at the LHC. All cuts and parameters are described in the text. The leading color adjustment procedure is applied. The LO distribution is rescaled by constant factor, to ensure that the LO and NLO normalizations coincide.

menters as tools for understanding properties of $W +$ jets process. In order to avoid too busy plots, we choose to only show leading order results computed with the “local” scale choice for the strong coupling constant in what follows. We stress that for all distributions the normalization of the leading order cross-section is adjusted to agree with next-to-leading order result. We show the distribution in transverse energy of the second-hardest and third-hardest jet in Figs. 5,6, rapidity of the hardest jet in Fig. 7 and the distribution in total transverse energy $H_{T,tot} = \sum_{\text{jets}} |p_{T,j}| + p_{T,l} + \cancel{p}_T$ in Fig.8. We also show leptonic distributions in Figs. 9 and 10 where we plot the lepton transverse momentum and the missing transverse momentum, respectively. As stated, in all considered cases local scales reproduce shapes of the distributions quite well.

III. $W + 3$ JET PRODUCTION AS A MODEL FOR BACKGROUND TO SUPERSYMMETRIC SEARCHES

In this Section we investigate QCD corrections to $W + 3$ jet production at the LHC for a set of cuts appropriate in supersymmetric searches. By construction, these background cuts seek to suppress the production of W bosons in association with jets as much as possible, effectively driving $W +$ jet production to corners of the available phase-space. It is therefore unclear if QCD radiative effects in those regions of phase-space are similar to QCD corrections to the production cross-sections discussed in the previous Section. To answer this question, we discuss two types of cuts, very similar to those suggested by the ATLAS and CMS collaborations, in their planned

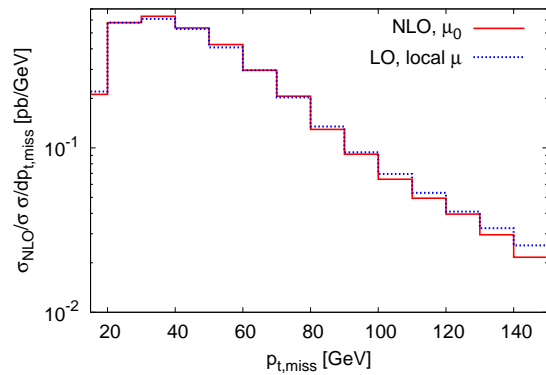


FIG. 10: The missing transverse momentum distribution for $W^+ + 3$ jet inclusive production cross section at the LHC. All cuts and parameters are described in the text. The leading color adjustment procedure is applied. The LO distribution is rescaled by constant factor, to ensure that the LO and NLO normalizations coincide.

searches for supersymmetry at the LHC.³ All the input parameters are the same as in the previous Section except that we use merging parameter $f = 0.7$ to define jets using SIScone algorithm.

A. ATLAS setup – faking jets from τ decays

We begin by considering cuts employed by the ATLAS collaboration to search for SUSY with R -parity conservation. In that case, the typical signal comes from gluino pair-production. If each gluino decays into two jets and a neutralino, a SUSY signature will involve 4 jets and missing transverse energy. A dominant background to this process comes from $Z + 4$ jet production, with the subsequent decay of the Z -boson into two neutrinos. Another important background comes from $W^+ + 3$ jet production⁴, followed by the decays $W^+ \rightarrow \bar{\tau}\nu_\tau \rightarrow \bar{\nu}_\tau\nu_\tau + \text{hadrons}$, so that hadrons from semileptonic decay of the τ lepton produce the fourth jet.

One can use peculiar kinematic properties of the fourth jet to connect it to τ decays and then reject such events but, because of limited efficiency in identifying τ decays and because the cross section for $W + 3$ jet production is almost two orders of magnitude larger than the $Z + 4$ jet

³ We point out that we kept cuts very similar to those used in the experimental studies done at 14TeV despite the fact that we use 10 TeV as center-of-mass energy. As a consequence cross-sections in this section are very small. A more realistic study would require adapting those cuts to the centre-of mass energy, but this is beyond the scope of this paper.

⁴ Clearly, there is also a similar background from $W^- + 3$ jet production but we do not consider it here.

production cross section, it is important to consider this source of the background as well.

We begin by listing a typical set of cuts that the ATLAS collaboration applies to suppress the $W \rightarrow \tau + 3j$ background [27, 28, 29]. First, all jets are required to have transverse momenta larger than 50 GeV and the transverse momentum of the leading jet should exceed 100 GeV. Second, missing energy in the event should satisfy $\cancel{E}_T > \max(100 \text{ GeV}, 0.2H_T)$ with $H_T = \sum_j p_{T,j} + \cancel{E}_T$. Third, no leptons with transverse momenta higher than 20 GeV should be present. Fourth, jets should be central $|\eta_j| < 3$. Finally, the event is required to be spherical and the cut $S_T > 0.2$ is applied on the transverse sphericity. We will not employ the sphericity cut in what follows because this observable is not collinear safe at parton level. In addition, since we consider semileptonic decays of the τ lepton, no high- p_T lepton is present in our events and we do not need to employ a 20 GeV lepton cut. The primary observable is the distribution in the effective mass H_T defined above and the range of a particular interest for SUSY searches, given existing bounds on gluino masses, is $H_T \gtrsim 1 \text{ TeV}$.

A clear exposition of the effect that the ATLAS cuts have on $W \rightarrow \tau + 3j$ background at leading order was recently given in Ref. [29]. It turns out that these cuts primarily change the normalization of the background but do not significantly affect the shape of the effective mass distribution, especially in the region $H_T \gtrsim 1 \text{ TeV}$. We would like to understand the impact of NLO QCD corrections to $W \rightarrow \tau + 3j$ on the H_T distribution. Our implementation of radiative corrections incorporates W decay to any leptonic final state but subsequent hadronic decays of the τ -lepton are not included. Yet, as we will argue now, this is not necessary if all we need is an estimate of the QCD effects.

We note that, given the above cuts and, in particular, the cut on the missing transverse energy, the τ lepton produced in W decays will be highly boosted and its decay products will be very collimated. We then completely neglect the angular distribution of the τ decay products and assume a perfect collinear splitting. If, in addition, we neglect all the spin correlations in τ decay $\tau \rightarrow \nu_\tau q_i \bar{q}_j$, we conclude that the neutrino has to carry away about a third of the τ momentum while the hadronic jet formed by a quark and an anti-quark from τ decay has to carry away two-thirds of the original τ momentum. We also expect that, since the τ lepton is highly boosted, all its hadronic decay channels will contribute to the same jet, making the inclusive treatment of jet properties a reasonable approximation.

We can implement this set up in our calculation by producing a W boson and letting it decay to a massless lepton and a massless neutrino. We then carry through all the steps required for the NLO QCD computation until the moment when the kinematics of events is examined and weights, relevant for various histogram bins, are calculated. At this point, we assign one-third of the lepton momentum to additional missing energy carried

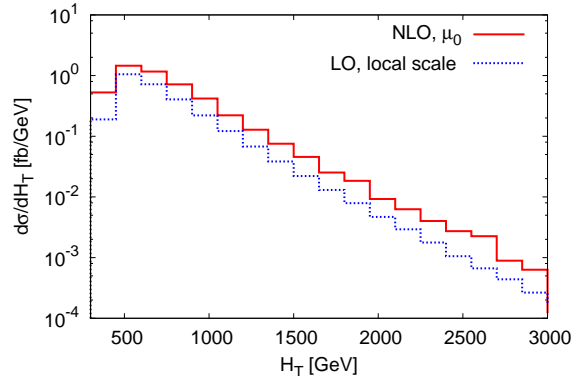


FIG. 11: Distributions in effective mass H_T for $(W^+ \rightarrow \bar{\tau}) + 3$ jet sample for ATLAS SUSY cuts described in the text. All cuts and parameters are described in the text. The leading color adjustment procedure is applied. The large difference between LO and NLO distributions can be absorbed by re-scaling the LO distribution by a constant factor.

away by ν_τ and two-thirds of the lepton momentum to the fourth (τ) jet in the event. Note that we do not apply the jet algorithm to check whether or not the hadronic jet from τ decay is sufficiently separated from the other three jets.⁵ Since this step is not necessary for infra-red safety, we feel that it is entirely justified to omit it, given the approximate nature of our analysis. For next-to-leading computations, we use the leading color adjustment procedure; we find that $\mathcal{R} = 0.93$ is an appropriate value of the re-scaling parameter for ATLAS cuts.

The results of our computation are presented in Fig. 11 where the LO H_T distribution for our default local scale compared to the NLO distribution for the factorization and renormalization scales set to μ_0 . We point out that the shape of the leading order distribution is similar to that obtained with Alpgen presented in Ref. [29], especially at high values of the effective mass. At lower values of the effective mass, there is a dependence on the modeling of $\tau \rightarrow$ hadrons transition and, given the very approximate nature of our procedure, it is not surprising that it tends to fail. It is reassuring, however, that our procedure seems to work quite well for high values of the effective mass.

As follows from Fig. 11, the H_T mass distribution receives *large positive* QCD corrections for ATLAS cuts. Note that distributions for local scales are *not* normalized to match the NLO distribution there. We studied the scale dependence of the leading order predictions by varying local scales around the central value by a factor of two. While we observe large $\sim \pm 50\%$ scale dependence in the LO result, the NLO QCD corrections are $\sim 100\%$

⁵ We did however impose a separation $R_{lj} = 0.5$ between the τ lepton and the jets.

and are thus considerably larger than what the LO scale variation suggests. The scale dependence of the H_{\perp} distribution does decrease considerably at NLO. We find that NLO QCD effects provide a universal enhancement of H_T distribution without distorting its shape. Interestingly, the cuts on jets and missing energy presented at the beginning of this Section have a similar impact on the $(W \rightarrow \tau) + 3$ jet background – each of the individual cuts reduces the magnitude of $(W \rightarrow \tau) + 3$ jet by a factor between three and four, without affecting the shape of the H_T distribution [29]. NLO QCD effects therefore are comparable to the effects of the cuts and work *in the opposite direction*.

We emphasize that, had we chosen scale μ_0 also in LO computation, we would observe large *positive* NLO QCD effects for H_{\perp} distribution, in sharp contrast with large *negative* corrections for such scale choice in high- $p_{\perp,j}$ regions, described in the previous Section (see Fig. 3). This is not surprising since, in contrast to $W + 3$ jet signal cuts, ATLAS cuts require large amount of missing energy, which forces W transverse momentum to be comparable or larger than transverse momenta of hard jets in the event. Jet branching on the other hand, can occur at lower relative transverse momenta. Taking the relative transverse momentum as the correct scale for the strong coupling constant, it is natural that LO cross sections for $\mu = \mu_0$ strongly underestimate the H_T distribution. This is indeed what we see when LO and NLO results are compared.

We believe that this discussion shows explicitly how problematic extrapolation from signal to background region can be since the NLO QCD effects for ATLAS cuts have no relation whatsoever to the NLO QCD effects for the total cross section. This mismatch happens because the kinematic region selected by ATLAS cuts gives negligible contribution to the total cross section. On the other hand, it appears that one can use low $H_T < 1$ TeV bins for ATLAS cuts to fix background normalization since QCD effects seem to be H_T -independent and SUSY contamination in low- H_T bins is small.

B. CMS indirect lepton veto cut

How robust is the situation discussed in connection with ATLAS cuts? To answer this question, we study another example of background cuts. Those cuts are adopted by the CMS collaboration for SUSY searches at the LHC [30, 31]. The target signal is gluino pair production and the final state involves jets and missing transverse energy.

The CMS collaboration does not veto leptons directly. Rather, cuts are designed in such a way that the contribution of W +jets becomes naturally small. Such cuts are usually referred to as *indirect lepton veto* cuts. We approximate the CMS indirect lepton veto cut by requiring that there are three or more jets in the event. The missing energy in the event should be large, $E_{\text{miss}} > 200$ GeV.

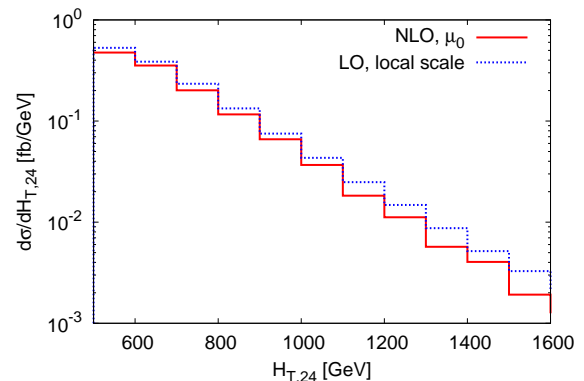


FIG. 12: Distributions in reduced transverse mass $H_{T,24}$ for $W^+ + 3$ jet events with CMS SUSY cuts that define indirect lepton veto procedure as described in the text. All cuts and parameters are described in the text. The leading color adjustment procedure is applied.

The leading jet in the event should be very central $|\eta_{\text{lead jet}}| < 1.7$ while all other jets should be in the central region $|\eta_{\text{other jets}}| < 3$. Jets are defined with the transverse momentum cut of $p_{T,j} > 30$ GeV but the transverse momentum of the leading and sub-leading jets should be larger than 180 and 110 GeV, respectively. Leptons from W decays should satisfy the same cuts as jets but lepton transverse momentum can not be the largest or next-to-largest in a particular event; experimentally, this requirement is implemented by cutting on the fraction of electromagnetic energy carried by a “jet”. Finally, a particular effective mass is required to be large

$H_{T,24} = \sum_{j=2}^4 p_{T,j} + E_{\text{miss}} > 500$ GeV. To calculate the sum in this formula one orders leptons and jets according to their hardness, disregards the leading jet and sums over transverse momenta of second-to-leading, third-to-leading and fourth-to-leading particles/jets.

We show the result of our computation of the NLO QCD corrections to the $W + 3$ jet cross section in case of CMS-style cuts in Figs. 12,13, where distributions in $H_{T,24}$ and missing energy are plotted. We again use μ_0 , as the factorization and renormalization scales and vary it by a factor two up and down to estimate scale uncertainties. The NLO corrections for these cuts change the LO result by -40% to -10% depending on the scale chosen in LO computations. For $\mu = \mu_0$, the corrections are about -10% and no significant changes of shape are observed. In this case, the scale variation at leading order gives a good indication of the size of NLO QCD corrections.

It is striking that the magnitude of NLO QCD corrections for CMS cuts is in strong contrast with the magnitude of NLO QCD effects for ATLAS cuts, discussed in the previous Section. This emphasizes the dependence of NLO QCD corrections on exact implementation of kine-

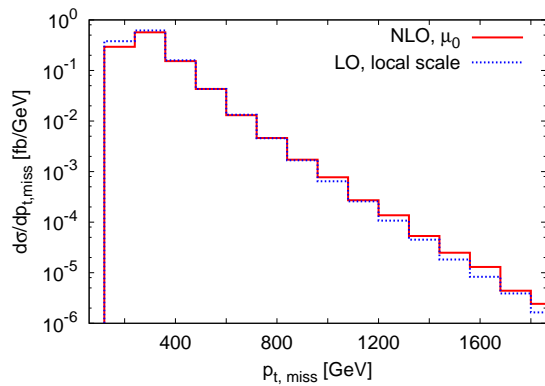


FIG. 13: Distributions in the missing transverse energy for $W^+ + 3$ jet events with CMS SUSY cuts that define indirect lepton veto procedure as described in the text. All cuts and parameters are described in the text. The leading color adjustment procedure is applied.

matic cuts even if such cuts are designed to target very similar physics beyond the Standard Model. On the other hand, we find that shapes of basic distributions employed in supersymmetric searches are described fairly well by leading order computations, for both ATLAS and CMS cuts. If one can verify that, say, low- H_\perp bins are not contaminated by New Physics, those bins can be used to determine the normalization of the background.

IV. CONCLUSIONS

We have discussed the NLO QCD corrections to $W + 3$ jet production at the LHC. We found that the inclusion of NLO QCD corrections leads to a significant reduction in dependence of LO results on the renormalization and factorization scales; the residual uncertainty associated with the total cross section is $\pm 5\%$. We showed that small corrections to total cross sections do not necessarily imply that corrections to differential distributions are small and there is a high degree of non-uniformity in these corrections across the available phase-space.

It should be stressed that the last statement depends upon renormalization and factorization scales chosen in leading order computations. In particular if leading order calculations are done with the scale $\mu = \sqrt{p_{T,W}^2 + m_W^2}$

we find a large difference in shapes between LO and NLO distributions. On the other hand, it is clear *a priori* that better results are achievable if scales are chosen based on local probabilities for jet branching. Here we have shown explicitly that when a local scale choice for the strong coupling constant is employed in leading order computations, such computations reproduce shapes of various NLO distributions quite well. Note that any leading order computation matched to parton shower in the spirit of CKKW procedure [39] *does* employ such local scales and our NLO analysis therefore confirms that, as far as shapes of various kinematic distributions are concerned, this is a very reasonable procedure.

The production of W -bosons in association with three jets is an important background for SUSY searches in jets + missing energy channels. We studied NLO QCD corrections to cuts employed by ATLAS and CMS collaborations for SUSY searches and found that such corrections are not at all correlated with corrections to the total cross sections. It is peculiar that the magnitude of NLO QCD corrections to, say, effective transverse mass distributions, is very different for ATLAS and CMS cuts in spite of the fact that these cuts are designed to serve the same purpose. We find large ($\sim 100\%$) corrections for ATLAS and small ($\sim 10\%$) QCD corrections for CMS cuts. We believe that this non-uniformity of corrections and their apparent strong dependence of the experimental set-up emphasizes the need for extending NLO QCD studies to other relevant backgrounds such as $W + 4$ jets and $Z + 3, 4$ jets. We hope that techniques for NLO QCD computations developed in recent years make such computations possible.

Acknowledgments We would like to thank Keith Ellis for collaboration at the early stages of this work, useful discussions and advice. We are grateful to Zoltan Kunszt, Fabio Maltoni, Michelangelo Mangano, Fulvio Piccinini and Gavin Salam for useful discussions and correspondence. Parts of this work were carried out during stays at Fermilab and CERN whose support and hospitality we gratefully acknowledge. K.M. is supported by NSF under grant PHY-0855365 and by the start up funds provided by Johns Hopkins University. G.Z. is supported by the British Science and Technology Facilities Council. Calculations reported in this paper were performed on the Homewood High Performance Cluster of Johns Hopkins University.

-
- [1] Z. Bern *et al.* [NLO Multileg Working Group], arXiv:0803.0494 [hep-ph].
 [2] A. Bredenstein, A. Denner, S. Dittmaier and S. Pozzorini, JHEP **0808**, 108 (2008) [arXiv:0807.1248 [hep-ph]].
 [3] A. Bredenstein, A. Denner, S. Dittmaier and S. Pozzorini, Phys. Rev. Lett. **103** (2009) 012002

- [arXiv:0905.0110 [hep-ph]].
 [4] R. K. Ellis, K. Melnikov and G. Zanderighi, JHEP **0904**, 077 (2009) [arXiv:0901.4101 [hep-ph]].
 [5] R. K. Ellis, K. Melnikov and G. Zanderighi, arXiv:0906.1445 [hep-ph].
 [6] C. F. Berger *et al.*, arXiv:0907.1984 [hep-ph].
 [7] C. F. Berger *et al.*, Phys. Rev. Lett. **102**, 222001 (2009)

- [arXiv:0902.2760 [hep-ph]].
- [8] G. Bevilacqua, M. Czakon, C. G. Papadopoulos, R. Pittau and M. Worek, arXiv:0907.4723 [hep-ph].
- [9] G. Passarino and M. J. G. Veltman, Nucl. Phys. B **160**, 151 (1979).
- [10] A. Denner and S. Dittmaier, Nucl. Phys. B **734**, 62 (2006) [arXiv:hep-ph/0509141].
- [11] G. Ossola, C. G. Papadopoulos and R. Pittau, Nucl. Phys. B **763**, 147 (2007) [arXiv:hep-ph/0609007].
- [12] G. Ossola, C. G. Papadopoulos and R. Pittau, JHEP **0803** 042 (2008) [arXiv:0711.3596 [hep-ph]].
- [13] Z. Bern, L. J. Dixon, D. C. Dunbar and D. A. Kosower, Nucl. Phys. B **425**, 217 (1994) [arXiv:hep-ph/9403226].
- [14] Z. Bern, L. J. Dixon, D. C. Dunbar and D. A. Kosower, Nucl. Phys. B **435**, 59 (1995) [arXiv:hep-ph/9409265].
- [15] Z. Bern, L. J. Dixon and D. A. Kosower, Nucl. Phys. B **513**, 3 (1998) [arXiv:hep-ph/9708239].
- [16] R. Britto, F. Cachazo and B. Feng, Nucl. Phys. B **725**, 275 (2005) [arXiv:hep-th/0412103].
- [17] R. K. Ellis, W. T. Giele and Z. Kunszt, JHEP **0803**, 003 (2008) [arXiv:0708.2398 [hep-ph]].
- [18] W. T. Giele, Z. Kunszt and K. Melnikov, JHEP **0804**, 049 (2008) [arXiv:0801.2237 [hep-ph]].
- [19] C. F. Berger *et al.*, Phys. Rev. D **78**, 036003 (2008) [arXiv:0803.4180 [hep-ph]].
- [20] W. T. Giele and G. Zanderighi, JHEP **0806**, 038 (2008) [arXiv:0805.2152 [hep-ph]].
- [21] C. F. Berger *et al.*, arXiv:0808.0941 [hep-ph].
- [22] R. K. Ellis, W. T. Giele, Z. Kunszt, K. Melnikov and G. Zanderighi, JHEP **0901**, 012 (2009) [arXiv:0810.2762 [hep-ph]].
- [23] A. Lazopoulos, arXiv:0812.2998 [hep-ph].
- [24] J. C. Winter and W. T. Giele, arXiv:0902.0094 [hep-ph].
- [25] A. van Hameren, C. G. Papadopoulos and R. Pittau, JHEP **0909**, 106 (2009) [arXiv:0903.4665 [hep-ph]].
- [26] See the LHC schedule at <http://lhc.web.cern.ch/lhc/>.
- [27] T. Yamazaki [ATLAS Collaboration and CMS Collaboration], arXiv:0805.3883 [hep-ex].
- [28] S. Yamamoto [ATLAS Collaboration], arXiv:0710.3953 [hep-ex].
- [29] M. L. Mangano, Eur. Phys. J. C **59** (2009) 373 [arXiv:0809.1567 [hep-ph]].
- [30] The CMS Collaboration Journ. Phys. G: Nucl. Part. Phys. **34** (2007), 995-1579.
- [31] M. Spiropulu, Eur. Phys. J. C **59**, 445 (2009).
- [32] See <http://mcfm.fnal.gov>.
- [33] S. Catani and M. H. Seymour, Nucl. Phys. **B485**, 291 (1997) [Erratum-ibid. **B** 510, 503; (1998)] [arXiv:hep-ph/9605323].
- [34] G. P. Salam and G. Soyez, JHEP **0705**, 086 (2007) [arXiv:0704.0292 [hep-ph]].
- [35] J. Pumplin, D. R. Stump, J. Huston, H. L. Lai, P. M. Nadolsky and W. K. Tung, JHEP **0207**, 012 (2002) [arXiv:hep-ph/0201195].
- [36] P. M. Nadolsky *et al.*, Phys. Rev. D **78**, 013004 (2008) [arXiv:0802.0007 [hep-ph]].
- [37] J. Alwall *et al.*, Eur. Phys. J. C **53**, 473 (2008) [arXiv:0706.2569 [hep-ph]].
- [38] C. W. Bauer and B. O. Lange, arXiv:0905.4739 [hep-ph].
- [39] S. Catani, F. Krauss, R. Kuhn and B. R. Webber, JHEP **0111**, 063 (2001) [arXiv:hep-ph/0109231].
- [40] M.L. Mangano, M. Moretti, F. Piccinini, R. Pittau, A. Polosa, JHEP **0307**:001, (2003).
- [41] G. Corcella, I.G. Knowles, G. Marchesini, S. Moretti, K. Odagiri, P. Richardson, M.H. Seymour and B.R. Webber, JHEP **0101** (2001) 010.